Available online at www.sciencedirect.com
ScienceDirect
Meat Science 77 (2007) 512–519
MEAT SCIENCE
www.elsevier.com/locate/meatsci

Dielectric behavior of beef meat in the 1–1500 kHz range: Simulation with the Fricke/Cole–Cole model

Jean-Louis Damez *, Sylvie Clerjon, Saïd Abouelkaram, Jacques Lepetit

INRA, UR370 QuaPA, F-63122 Saint Genès Champanelle, France

Received 15 November 2006; received in revised form 27 April 2007; accepted 27 April 2007

Abstract

The electrical properties of biological tissues have been researched for many years. Impedance measurements observed with increasing frequencies are mainly attributed to changes in membrane conductivity and ion and charged-molecule mobility (mainly Na^+, K^+, CL^- ions). Equivalent circuits with passive electrical components are frequently used as a support model for presentation and analyses of the behavior of tissues submitted to electrical fields. Fricke proposed an electrical model where the elements are resistive and capacitive. The model is composed of a resistive element (Rp) representing extracellular fluids (ECF) placed in parallel with a capacitive element (Cs) representing insulating membranes in series and a resistive element (Rs) representing intracellular fluids (ICF). This model is able to describe impedance measurements: at lower frequencies, most of the current flows around the cells without being able to penetrate them, while at higher frequencies the membranes lose their insulating properties and the current flows through both the extracellular and intracellular compartments. Since meat ageing induces structural change, particularly in membrane integrity, the insulating properties of membranes decrease, and intracellular and extracellular electrolytes mix, thus driving changes in their electrical properties. We report a method combining the Fricke and Cole–Cole models that was developed to monitor and explain tissues conductivity changes in preferential directions during beef meat ageing.

Keywords: Dielectric properties; Electrical conduction; Biomathematics; Inverse modeling; Membrane; Beef ageing; Muscle structure

1. Introduction

Electrical impedance measurement techniques are rapid, straightforward and cost-effective. Many teams attempted to link electrical parameters to physical, chemical or biological characteristics (Pethig & Kell, 1987; Foster & Schwan, 1989; Valentinuzzi, Morucci, & Felice, 1995), thus generating practical applications in the food industry (Bauchot, Harker, & Arnold, 2000; Varlan & Sansen, 1996; Chevalier, Ossart, & Ghommidh, 2006), particularly in the meat sector (Damez, Clerjon, Abouelkaram, & Lepetit, 2006; Lepetit, Salé, Favier, & Dalle, 2002; Swatland, 1997; Whitman, Forrest, Morgan, & Okos, 1996). The majority of the structural and functional properties of biological tissues can be determined by interpreting data on electric and dielectric properties (Schwan & Takashima, 1993). The prevalent phenomena at the microscopic scale are flow of ionic charges, interface polarization, and the relaxation phenomena produced by dipolar rotation and rotation of parts of macromolecules.

Three areas of dispersion are denoted α, β and γ according to the Schwan classification describing these three frequency bands (Schwan, 1957). The majority of biological tissues fit this spectral pattern shown in Fig. 1.

In the literature, although the three frequency bands are not always linked to particular biophysics phenomena, dispersion is nevertheless caused by relaxation phenomena (Pethig, 1979; Pethig & Kell, 1987). The γ-dispersion observed at high frequency (such as above 100 MHz) is

* Corresponding author. Tel.: +33 4 73 62 41 87; fax: +33 4 73 62 40 89.
E-mail address: damez@clermont.inra.fr (J.-L. Damez).

0309-1740/$ - see front matter © 2007 Elsevier Ltd. All rights reserved.
doi:10.1016/j.meatsci.2007.04.028

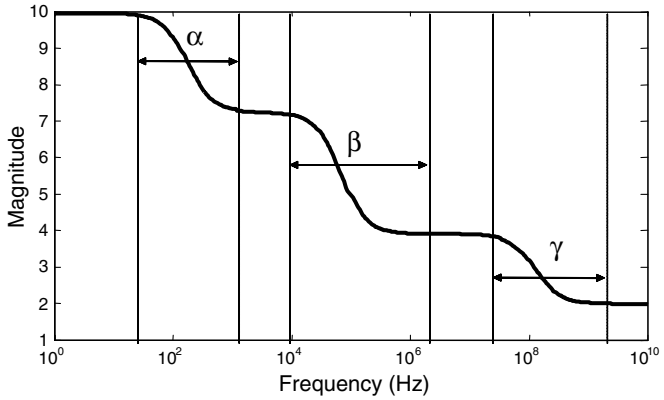

Fig. 1. Hypothetical frequency impedance diagram of biological tissue.

mainly due to the permanent dipole relaxation of small molecules, as in water molecules which are predominant in biological tissues.

The β-dispersion covers an intermediate frequency band ranging from a few kHz up to a few dozen MHz. These relaxation phenomena are sample-dependent and caused by the Maxwell–Wagner effect. These phenomena appear in inhomogeneous materials (e.g. suspensions of cells in liquid) and are due to interface polarization (Hanai, 1960). According to the Schwan classification, myoglobin aqueous solutions for example have relaxation frequencies between 105 and 107 MHz (Pethig & Kell, 1987). Although it is clearly a β-dispersion, this relaxation phenomenon is of the same nature as those of the γ-dispersion for small molecules. These cases can nevertheless be compared to those of the γ-dispersion, but the relaxation that occurs is not due to permanent dipoles but to electrical charges induced by electric fields. The first theoretical study was led by Pauly and Schwan (1959) and was later complexified by Asami, Hanai, and Koizumi (1980). Schwan showed that very rigorous measurements highlight a partial overlap of the relaxation phenomena in the β-dispersion area that can, in part, be attributed to the Maxwell–Wagner effects of the intracellular structures. This led some authors to split the β-dispersion area into two sub-dispersion areas, β_1 and β_2 (Asami & Yonezawa, 1996). As reported by Pliquett, Altmann, Pliquett, and Schöberlein (2003), the β-dispersion area is a direct measure of the cell membrane behavior. The corresponding 1–1500 kHz range observation could serve in the study of cells membrane integrity during meat ageing: myofiber membrane acting as a dielectric insulator whose insulating properties decrease with ageing, oxidation of the phospholipid membrane layers and lysis occurring after the cell death making the membrane porous.

The α-dispersion, which occurs at low frequencies, expresses the relaxation of the "non-permanent" dipoles which are formed during ionic flow across cell surfaces or large molecules. This phenomenon is described in detail in Pethig and Kell (1987), and an ideal model for α-dispersion and β-dispersion was developed by Gheorghiu (1993, 1994) and later adapted to the mesostructural characterization of animal tissues (Damez, Clerjon, & Abouelkaram, 2005). The spectrum range corresponding to low frequencies (α range) has been extensively studied in biomedical applications on the monitoring of tissue or organ vitality for transplantation. Research has highlighted the presence of interfaces and compartments at a microscopic scale (1–10 μm) (Gheorghiu, 1993, 1994; Gersing, Hofmann, Kehrer, & Pottel, 1995). From an electric point of view, ECF and ICF can be regarded as electrolytes. Na^+ and Cl^- ions are by far in extracellular fluids (ECF) (142 mEq/L and 105 mEq/L, respectively). In intracellular fluids (ICF), K^+ is major intracellular cation (100 mEq/L), while phosphate ($PO4^-$, 142 mEq/L) and proteins (55 mEq/L) are major intracellular anions. Osmotic load is similar between intracellular medium and extracellular medium (205 mEq/L against 154 mEq/L) (Crenshaw, 1991). The charge carriers are K^+ ions, proteins and organic acids. Thus, the electrical properties are dependent on the physical and chemical parameters determining the concentration and mobility of ions within metabolic fluids.

2. Modeling approach: the Cole–Cole and Fricke models

The Cole models are founded on the basis of the description given in Cole and Cole (1941). The impedance Z^* is a complex function of alternating current frequency f, e.g.

$$Z^* = Z_{\text{real}} + iZ_{\text{imag}}$$

were Z_{real} is the real part, Z_{imag} the imaginary part and $i = (-1)^{1/2}$.

Each dispersion range (e.g. the β-dispersion) can be fitted by a Cole–Cole equation.

The Cole–Cole equation is:

$$Z^* = R_\infty + \frac{(R_0 - R_\infty)}{1 + (i\omega\tau)^{1-\alpha}} \quad (1)$$

where $\omega = 2\pi f$, R_0 and R_∞ are the impedance at very low and very high frequency, respectively, τ is the time constant and the dimensionless exponent α (taking values between 0 and 1) is a constant correcting the non-strict capacitive behavior of membranes due to dielectric losses, and reflecting distribution in dispersion.

The Cole–Cole plot according to these models is made in a complex Nyquist plane. The impedance locus forms a semicircular arc located below the real axis. If material inhibits multi-relaxation ranges, the plot presents semicircular multi-arcs, as shown on Fig. 2.

A standard way to facilitate the interpretation and modeling of these phenomena is to consider biological tissue as being constituted of a more or less homogeneous suspension of cells in an ionized liquid medium. The model described by Fricke (Fricke & Morse, 1924; Fricke, 1925; Fricke & Morse, 1926) assimilates biological tissue components (cells, liquid, membranes, intracellular (ICF) and extracellular fluids (ECF)) with passive electrical elements (resistor, capacitor) connected in series and in parallel

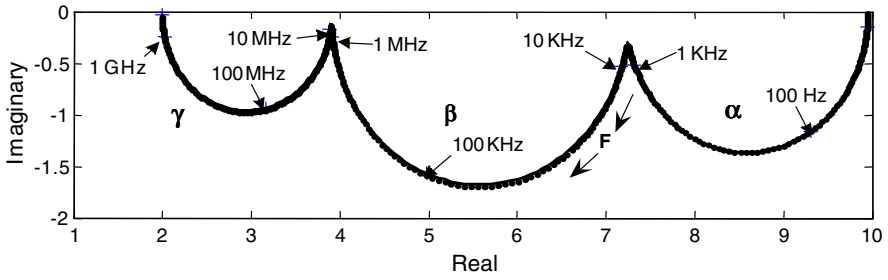

Fig. 2. Hypothetical Cole–Cole impedance plot of biological tissue showing the 3 overlapping dispersions of α, β and γ ranges.

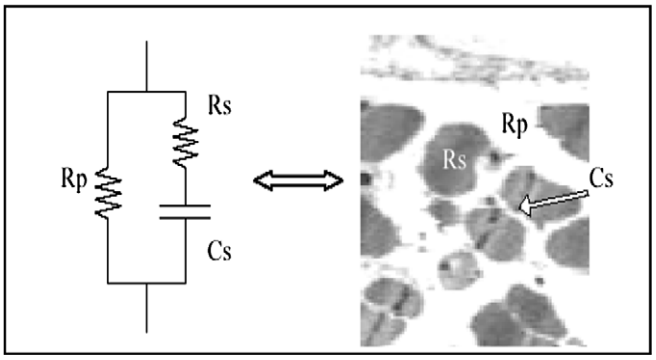

Fig. 3. Electrical Fricke model with equivalent resistances Rs (ICF), Rp (ECF) and cell membrane capacitance, Cs.

(Fig. 3). The Fricke model has been widely used to quantify cells or micro-organisms in suspension in a liquid medium, and can also be used in homogeneous mediums.

In this model, Rp and Rs represent the resistances of ECF and ICF, respectively, while Cs is the cell membrane capacitance. The Fricke model can be combined with a Cole–Cole model to study ageing in meat, which is an anisotropic medium (Damez et al., 2005).

Based on the Fricke model, the parameters in the Cole–Cole equation are:

$$\tau = (\mathrm{Rs} + \mathrm{Rp})\mathrm{Cs}, \quad R_0 = \mathrm{Rp} \quad \text{and} \quad R_\infty = \frac{\mathrm{Rp\ Rs}}{\mathrm{Rp} + \mathrm{Rs}} \tag{2}$$

Following the Moivre transformation of a complex number:

$$(i\omega\tau)^n = (\omega\tau)^n[\cos(n\pi/2) + i\sin(n\pi/2)] \tag{3}$$

the impedance components of Z^* in Eq. (1) can be broken down into:

$$Z_{\mathrm{real}} = \frac{\mathrm{Rp\ Rs}}{\mathrm{Rp} + \mathrm{Rs}} + \frac{\mathrm{Rp}[1 + (\omega\tau)^{1-\alpha}\cos((1-\alpha)\pi/2)]}{[1 + (\omega\tau)^{1-\alpha}\cos((1-\alpha)\pi/2)]^2 + [(\omega\tau)^{1-\alpha}\sin((1-\alpha)\pi/2)]^2}$$
$$Z_{\mathrm{imag}} = -\frac{\mathrm{Rp}(\omega\tau)^{1-\alpha}\sin((1-\alpha)\pi/2)}{[1 + (\omega\tau)^{1-\alpha}\cos((1-\alpha)\pi/2)]^2 + [(\omega\tau)^{1-\alpha}\sin((1-\alpha)\pi/2)]^2} \tag{4}$$

The Fricke model, although highly elementary, remains an excellent method for giving a simple description of biological environments at microscopic level. However, it is still necessary to make it more complex by adding resistive and capacitive elements, whereas the level of structure to be described is itself more complex (Geddes & Bake, 1967).

3. Experimental procedure

The experiments were carried out on a population of 104 samples obtained from 7 *Semimembranosus* (SM), 12 *Rectus Abdominis* (RA), 7 *Semitendinosus* (ST) muscles of cull cows (Friesian and Holstein cows, about 6 years of age). Each muscle was divided into 4 pieces, in order to perform measurements on each muscle at 4 *postmortem* times: 2 days *postmortem*(D2), 3 days *postmortem*(D3), 6 days *postmortem* (D6), and at 14 days *postmortem*(D14). Measurements were taken three times on each sample with two directions of the electric field according to fibers direction, taking the whole number of tests to 624 observations. An observation consisted of the acquisition of an impedance spectrum with 80 frequencies following a logarithmic law, between 1 kHz and 1500 kHz. Muscles excised 1 h after slaughter were vacuum-packed and stored for 24 h in water at 15 °C in order to avoid cold shortening. Subsequently and throughout the study, the vacuum-packed meat samples were stored in a chilled room (4 °C) between measurements. Measurements were taken at 4 ± 1 °C at 2 days (D2), 3 days (D3), 6 days (D6) and 14 days (D14) *postmortem*.

Impedance measurements were carried out using a probe consisting of 2 stainless steel electrodes spaced 5 cm apart ($\phi = 0.6$ mm; $L = 5$ mm), making it possible to take measurements both longitudinally and transversally to the fiber direction, and were recorded on a HP 4194A

Impedance/Gain-Phase analyzer (Hewlett-Packard Company, San Fernando, CA) scanning 80 frequencies ranging from 1 kHz to 1500 kHz. Resistive and capacitive electrical properties were modelled using an adapted Cole–Cole relaxation equation (2) (Cole & Cole, 1941; Foster & Schwan, 1989).

For model fitting, we implemented an improved algorithm from the *fminsearch* function of Matlab R14 based on a Nedler–Mead simplex method (Nedler & Mead, 1965). This model fitting gives good results as it performs a fit on each data set (both on real part and imaginary part).

4. Results and discussion

Electrical modeling was performed on each of the 104 samples at 4 *postmortem* times. Fig. 4 illustrates typical Cole–Cole plots from early postmortem (2 days (D2) after slaughter) to ageing (14 days (D14) after slaughter) of a *Rectus Abdominus* bovine muscle (all samples yielded similar patterns). The measurements both along myofibers (electrodes located longitudinally to the myofiber axis) and across myofibers (electrodes transversally to the myofiber axis) are given.

The plots traced a semicircular arc confirming the electrical behavior advanced by Cole. Impedance at high frequencies (in this instance at 1.5 MHz) tended to be similar for both transversal and longitudinal directions, both early on and after ageing. This reflects that myofiber membranes act as capacitance and that the dielectric anisotropy disappears at high frequencies.

There was different impedance at low frequencies according to measurement direction, with impedance being higher across the myofiber axes than along them, as previously reported by other authors (Lepetit et al., 2002; Swatland, 1980). This may reflect the longer pathway of the electric fields across the myofibers. For a same distance D between the measurement electrodes, the pathway across the myofibers is about $\pi/2$ longer than along the myofiber axe if the myofiber section is assumed to be a circle, with electric fields circumventing the circular myofiber membranes following N half-circle in transverse myofiber measurements whereas they follow a distance equivalent to N myofiber diameters (d) in the case of longitudinal myofiber measurements. Hence, for the same distance between electrodes, length of electric fields across myofibers was $P1 = N(\pi/2 \cdot d)$ and length of electric fields along myofibers was $P2 = N \cdot d$. Since impedance is distance-dependent, the distance pathways of electric fields acted on impedance in the same manner. The factor $P1/P2$ between transverse and longitudinal impedance measurements is close to $\pi/2$, which is consistent with other reports (Lepetit et al., 2002; Swatland, 1980), thus confirming our hypotheses on the behavior of electric

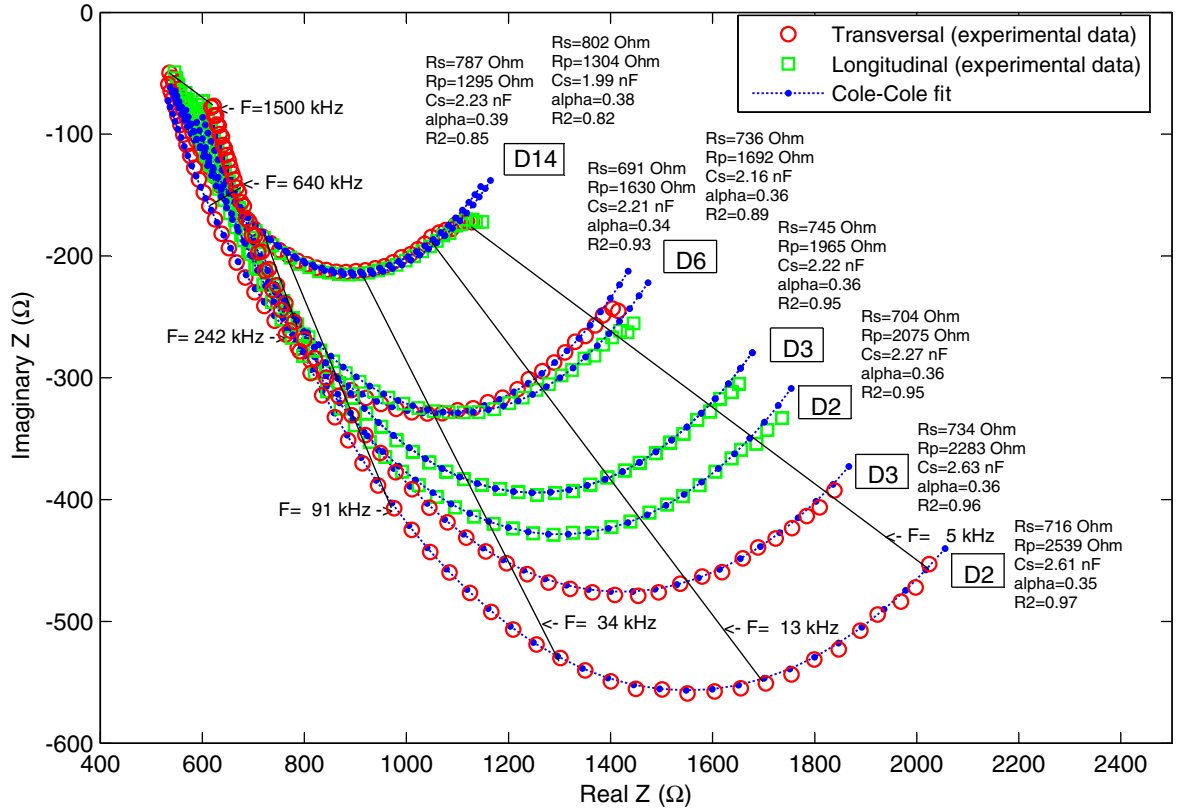

Fig. 4. Typical plots of imaginary part against real part of impedances for individual *Rectus Abdominus* (RA) beef muscle samples, after 2 days (D2), 3 days (D3), 6 days (D6) and 14 days (D14) of ageing. Impedance measurements were taken longitudinally and transversally to the muscle fiber direction.

fields at low frequencies circumventing the myofiber membranes. However, this $\pi/2$ factor has never before been highlighted.

From (D2) to (D14), the diameters of the plot arcs contract, indicating that the electrical impedances reduce and lead to better conductivity, which suggests shorter electrical fields lengths and improved ions mobility. In the same time, the transversal and longitudinal impedance plots tend to superimpose, which is evidence of the same electrical behavior. This reflects that, after cell death and during ageing, ECF and ICF mix due to the permeability of cell membranes. During ageing, it is estimated that between 60 and 80% of the increase in osmotic pressure is driven by metabolites, and the remainder by free inorganic ions not present in the cytoplasm before the *rigor mortis* (Winger, 1979; Wu & Smith, 1987; Bonnet, Ouali, & Kopp, 1992). These ions, which are concentrated in organoids such as the sarcoplasmic reticulum and mitochondria, are released after the death of the animal during depolarization of the membranes (Ouali et al., 2006). Feidt and Brun-Bellut (1996) showed that the release of Na^+, K^+, and Cl^- ions over time was not only pH-dependent but was also directly affected by cellular death, in particular the rupture of membranes. In addition, Mg^{++} and Ca^{++} are fragmented ions related to proteins. Thus, even released out of the sarcoplasmic reticulum after exhaustion of the ATP and inactivation of membrane pumps, these two ions can still bind to proteins with which they have a strong affinity. The final quantities of free Mg^{++} and Ca^{++} thus appear to be mainly conditioned by pH. When the pH approaches the pI of myofibrillar proteins (i.e. around pH 5), the protein charge tends to be cancelled and their capacity to adsorb cations decreases. A lower pH leads to more slacking of the two ions. Based on the study of Feidt and Brun-Bellut (1996), it is possible to distinguish passive fixing of the ions by proteins, which is directly dependent on pH, and active bulkheading, which stops as the cell's energy reserves are exhausted. The relative contributions of these two phenomena to the ion release will vary according to the ions involved. The ionic flow across cell surfaces or large molecules allow the formation of "non-permanent" dipoles witch are expressed in the the α-dispersion range, that can be observed at lower frequencies and at 14 days of ageing (D14) in Fig. 4: the semicircular plots tend to plateau out, indicating that the border between α and β area appears at around 15 kHz, as early described in Schwan (1957).

Impedances parameters (Rp, Rs and Cs) are calculated from fittings of the transversal and longitudinal plots according to the Fricke model. The three parameters are capacitance Cs, which reflects the state of myofibers membranes, and the two resistances Rs and Rp, which reflect ICF and ECF conductivities, respectively. These parameters Cs, Rs and Rp versus time *postmortem* are plotted on Figs. 5–7, for the 3 types of muscles studied (respectively for *Rectus Abdominis* (RA), for *Semitendinosus* (ST), and for *Semimembranosus* (SM) muscles).

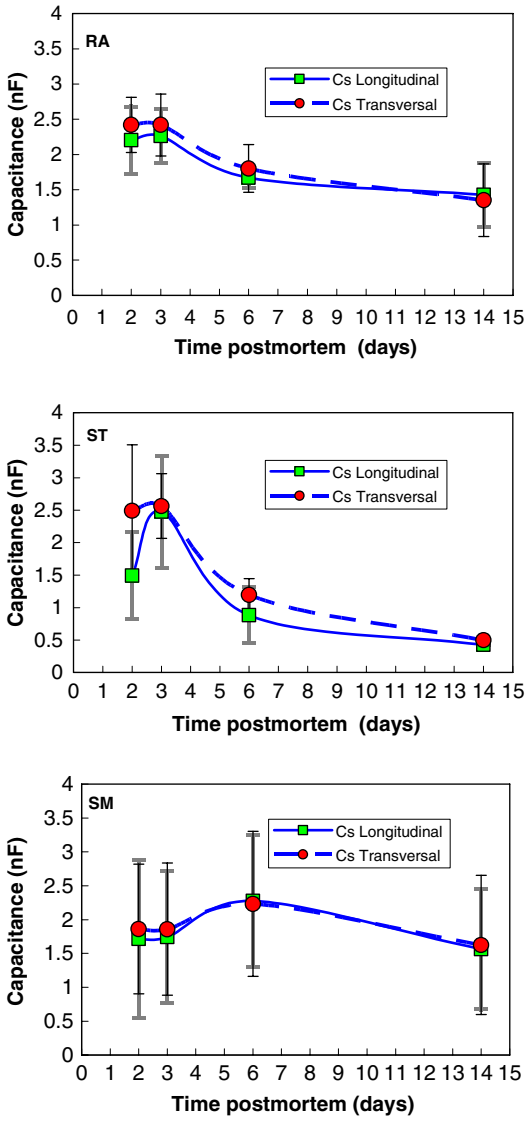

Fig. 5. Evolution of dielectric parameter Cs versus time *postmortem* for the 3 types of muscles studied (respectively for *Rectus Abdominis* (RA), for *Semitendinosus* (ST), and for *Semimembranosus* (SM) muscles).

The plot of capacitance Cs arising from cell membranes is shown in Fig. 5. The curves level out during ageing, reaching very similar values for both longitudinal and transversal measurements. This confirms that the myofiber membrane acts as a dielectric insulator whose insulating properties decrease with ageing. This may be due to oxidation of the phospholipid membrane layers and lysis occurring after the cell death (Huff-Lonergan & Lonergan, 2005), making the membrane porous.

Rs rises steadily with ageing (Fig. 6), giving very similar values in both the longitudinal and transversal directions. This denotes that electric fields across the myofibers (in intracellular compartments) meet relatively more insulating stuffs as ageing progresses. This can be explained by shrinkage of myofibers during the postmortem period which causes exudation of electrolytes from cells, with the remaining nuclei acting as insulators inside the cells (Valet, Silz,

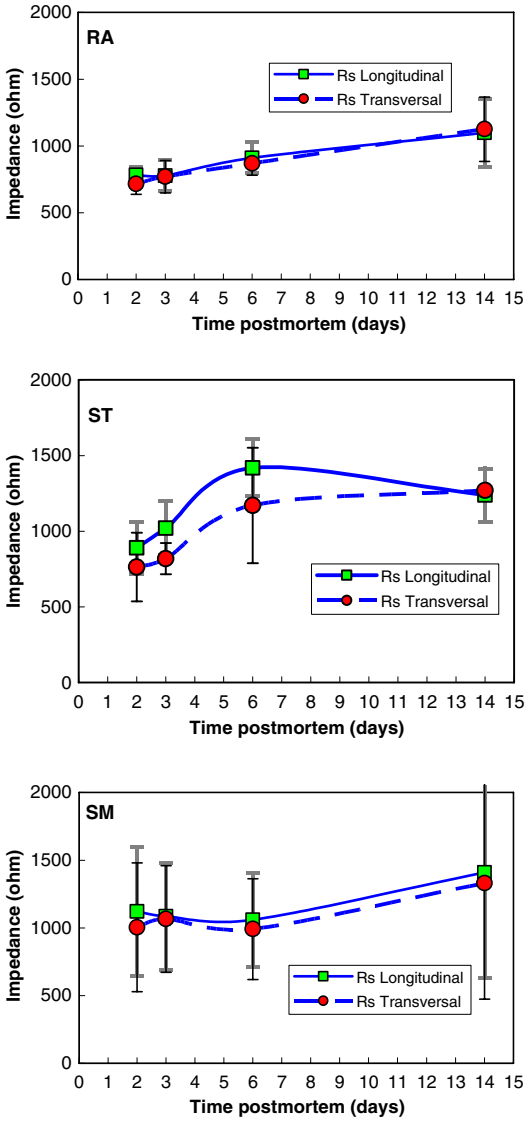

Fig. 6. Evolution of impedance parameter Rs versus time *postmortem* for the 3 types of muscles studied (respectively for *Rectus Abdominis* (RA), for *Semitendinosus* (ST), and for *Semimembranosus* (SM) muscles).

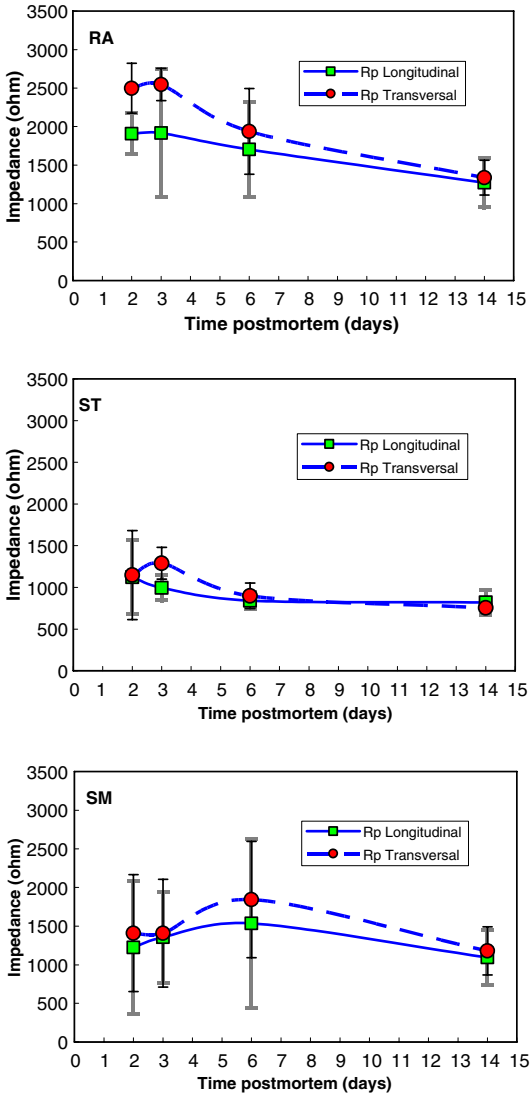

Fig. 7. Evolution of impedance parameter Rp versus time *postmortem* for the 3 types of muscles studied (respectively for *Rectus Abdominis* (RA), for *Semitendinosus* (ST), and for *Semimembranosus* (SM) muscles).

Metzger, & Ruhenstroth-Bauer, 1975). Rs may, therefore, reflect myofibers shrinkage during ageing.

Rp decreased with ageing (Fig. 7), and Rp was much higher in the transversal than the longitudinal direction during the early stages of ageing, as previously underlined for impedance. This confirms that electric fields preferably travel through ECF before ageing, since the higher transversal Rs results from a longer circumventing path taken by electrical fields compared to longitudinal Rs and its straight electrical field path. During ageing, ECF and ICF progressively mix, electrolyte conductivity increases, and thus resistivity decreases to reach the same value for both directions, meaning that meat is no longer electrically anisotropic after the membrane disruption that occurs during ageing, confirming the results of Lepetit, Damez, Moreno, Clerjon, and Favier (2001).

Cole–Cole plots at D2 time for the muscle types studied are shown in Fig. 8. Comparing the electrical impedances parameters (Rp, Rs and Cs) with muscle types (RA, ST and SM), RA and ST highlights more differences between longitudinal and transversal values of electrical impedance parameters than for SM muscle as showed on Figs. 5–7. This could be caused by the more fiber aligned structure of RA and ST muscles. RA and ST muscles differ from SM as they differ in speed of maturation (Geesink, Ouali, & Smulders, 1992; Ouali et al., 2005) with the slowest speed for RA. This difference in speed of maturation was explained by these authors by the proteolysis of myofibrillar proteins and the disintegration of the myofibrillar structure depending on the osmotic pressure attained in post-rigor muscle, explaining it also in terms of membrane degradation.

For all types of muscles, longitudinal impedance curves are upon transversal impedance curves, indicating that longitudinal impedances are lowers than transversal impedances before ageing as reported in Lepetit et al.

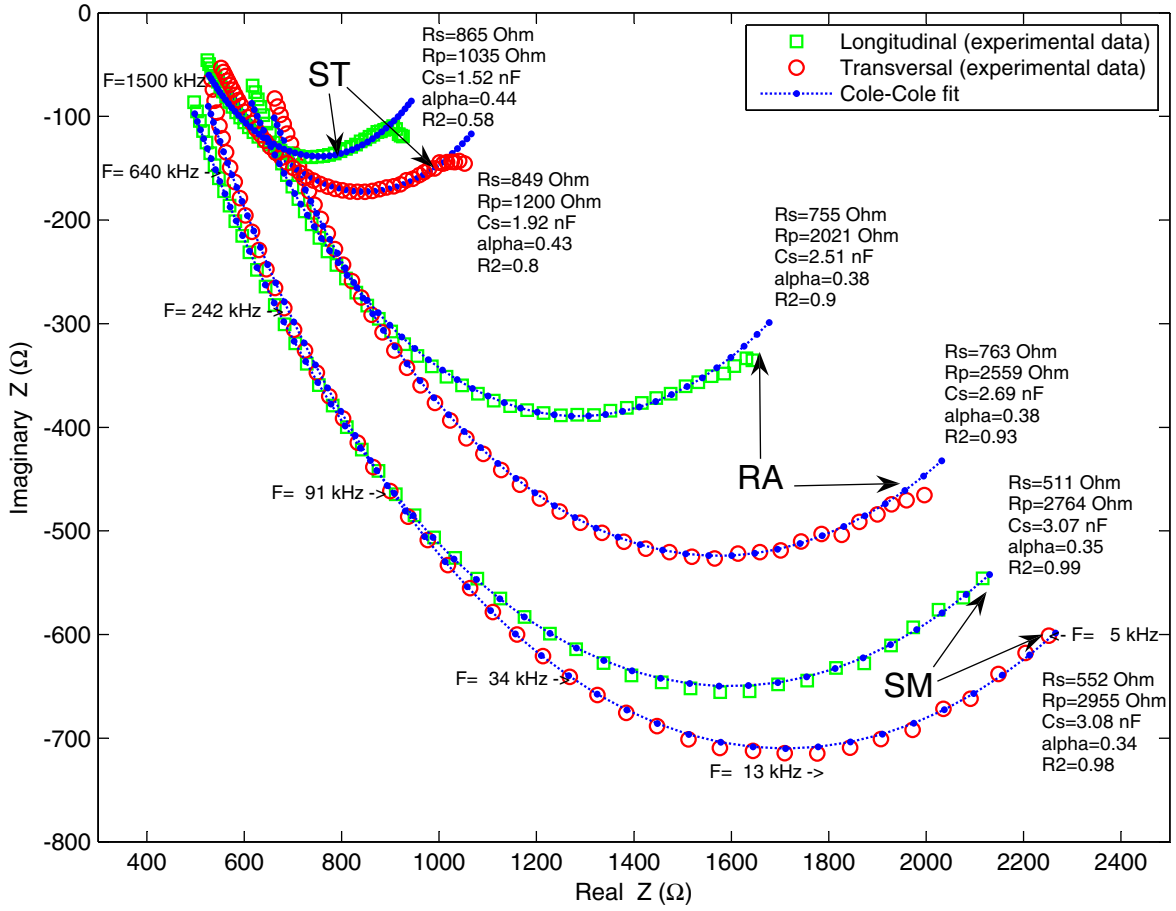

Fig. 8. Typical plots of imaginary part against real part of impedances for *Rectus Abdominis* (RA), for *Semitendinosus* (ST), and for *Semimembranosus* (SM) beef muscles, after 2 days (D2) of ageing. Impedance measurements were taken longitudinally and transversally to the muscle fiber direction.

(2002) and Swatland (1980). Impedances plots show different arcs, the shorter for ST muscles, the longer for SM muscles, suggesting once again that meat impedance is muscle dependant, as previously reported in Lepetit et al. (2002).

5. Conclusions

This study highlights how Polar Impedance Spectrometric study of biological tissues, in this case meat, generates a battery of useful data on the structural organization and the biological and physical state of various components. At low frequency, anisotropy is strongly marked: the impedance in the direction transverse to the grain of the muscle fibers is roughly $\pi/2$ times that observed in the longitudinal direction. The anisotropy disappears at high frequency, since the cellular membranes no longer act as electrical barriers; thus, at high frequency, impedance only reflects the characteristics of the intra- and extra-cellular media. Since meat is electrically anisotropic, measurements were carried out in two directions: along or across the myofibers. Myofibrillar membrane integrity is reflected by capacitance Cs, while the conductivity of extracellular fluid and intracellular fluids was estimated using Rp and Rs resistances. The behavior of these three parameters during meat ageing has been discussed. The capacitance Cs decreases according to membranes lysis and oxidation of the phospholipid membrane layers. Rp decreases due to increasing flow of free ions and increasing volume of extracellular compartments and Rs decreases because of ICF exudation that increases concentration of insulating stuff in cells. Experimental studies applying dielectric spectroscopy to beef meat were carried out in the β-range (1–1500 kHz) which is known to reflect dielectic properties of biological interfaces, and the dispersions observed were described using a simple model based on the Cole–Cole and Fricke models. However, the model used here has to be made more complex by adding resistive and capacitive elements when the level of structure to be described is itself more complex. By tracking variations in impedance according to the angle between the electrical field direction and the main direction of fibres, the results demonstrate that a measurement of structural state, and thus of maturation state of meat, could be obtained. This study leads toward the design of a sensor giving the state of maturation that could be used in a meat industry setting, based on the measure of impedances parameters and electrical anisotropy properties of meat.

References

Asami, K., Hanai, T., & Koizumi, N. (1980). Dielectric approach to suspensions of ellipsoidal particles covered with a shell in particular reference to biological cells. *Japanese Journal of Applied Physics, 19*, 359.

Asami, K., & Yonezawa, T. (1996). Dielectric behavior of wild-type yeast and vacuole-deficient mutant over a frequency range of 10–10 GHz. *Biophysical Journal, 71*, 2192–2200.

Bauchot, A. D., Harker, F. R., & Arnold, W. M. (2000). The use of electrical impedance spectroscopy to assess the physiological condition of kiwifruit. *Postharvest Biology and Technology, 18*, 9–18.

Bonnet, M., Ouali, A., & Kopp, J. (1992). Beef muscle osmotic pressure as assessed by differential scanning calorimetry (DSC). *International Journal of Food Science and Technology, 27*, 399–408.

Chevalier, D., Ossart, F., & Ghommidh, C. (2006). Development of a non-destructive salt and moisture measurement method in salmon (Salmo salar) fillets using impedance technology. *Food Control, 17*, 342–347.

Cole, K. S., & Cole, R. H. (1941). Dispersion and absorption in dielectrics. I. Alternating current characteristics. *The Journal of chemical physics, 9*, 341–351.

Crenshaw, T. D. (1991). Sodium, potassium, magnesium and chloride in swine nutrition. In E. R. Miller, D. E. Ullrey, & A. J. Lewis (Eds.), *Swine nutrition*. Stoneham, MA: Butterworth.

Damez, J. L., Clerjon, S., & Abouelkaram, S. (2005). Mesostructure assessed by alternating current spectroscopy during meat ageing. In *Proceedings of the 51st international congress of meat science and technology* (pp. 327–330).

Damez, J. L., Clerjon, S., Abouelkaram, S., & Lepetit, J. (2006). Polarimetric ohmic probes for the assessment of meat ageing. In *Proceedings of the 52nd international congress of meat science and technology* (pp. 637–638).

Feidt, C., & Brun-Bellut, J. (1996). Estimation de la teneur en ions libres du Longissimus Dorsi lors de la mise en place de la rigor mortis chez le chevreau. *Vièmes Journées des Sciences et Technologie de la Viande, Clermont-Ferrand, Viandes et Produits Carnés, 17*, 319–321.

Foster, K. R., & Schwan, H. P. (1989). Dielectric properties of tissues and biological materials, a critical review. In *Critical reviews in biomedical engineering* (pp. 25–104). Boca Raton, FL: CRC Press.

Fricke, H., & Morse, S. (1924). A mathematical treatment of the electrical conductivity and capacity of disperse systems. I. The electric conductivity of a suspension of homogeneous spheroids. *Physical Review, 24*, 575–587.

Fricke, H. (1925). A mathematical treatment of the electric conductivity and capacity of disperse systems. II. The capacity of a suspension of conducting spheroids by a non-conducting membrane for a current of low frequency. *Physical Review, 26*, 678–681.

Fricke, H., & Morse, S. (1926). The electric capacity of tumors of the breast. *Journal of Cancer Research, 10*, 340–376.

Geddes, L. A., & Bake, L. E. (1967). The specific resistance of biological material – a compendium of data for the biomedical engineer and physiologist. *Medical & Biological Engineering, 5*, 271–293.

Geesink, G. H., Ouali, A., & Smulders, F. J. M. (1992). Tenderization, calpain/calpastatin activities and osmolality of 6 different beef muscles. In *Proceedings of the 38th international congress of meat science and technology* (pp. 363–366).

Gersing, E., Hofmann, B., Kehrer, G., & Pottel, R. (1995). Modelling based on tissue structure: The example of porcine liver. *Innovation et Technologie en Biologie et Médecine, 16*, 671–678.

Gheorghiu, E. (1993). The dielectric behaviour of a biological cell suspension. *Romanian Journal of Physics, 38*, 113–117.

Gheorghiu, E. (1994). The dielectric behaviour of suspensions of spherical cells: A unitary approach. *Journal of Physics A: Mathematical and General, 27*, 3883–3893.

Hanai, T. (1960). Theory of the dielectric dispersion due to the interfacial polarization and its application to emulsions. *Kolloid-Z, 171*, 23–31.

Huff-Lonergan, E., & Lonergan, S. M. (2005). Mechanisms of water-holding capacity of meat: The role of postmortem biochemical and structural changes. *Meat Science, 71*, 194–204.

Lepetit, J., Damez, J.L., Moreno, M.V., Clerjon, S., & Favier, R. (2001). Electrical anisotropy of beef meat during ageing. In *Proceedings of the 47th international congress of meat science and technology*.

Lepetit, J., Salé, P., Favier, R., & Dalle, R. (2002). Electrical impedance and tenderisation in bovine meat. *Meat Science, 60*, 51–62.

Nedler, J. A., & Mead, R. (1965). A simplex method for function minimization. *Computer Journal, 7*, 308–313.

Ouali, A., Sentandreu, M. A., Aubry, L., Boudjellal, A., Tassy, C., Geesink, G. H., et al. (2005). Meat toughness as affected by muscle type. In J. F. Hocquette & S. Gigli (Eds.), *Indicators of milk and beef quality* (pp. 391–396). Wageningen, The Netherlands: Wageningen Academic Publishers, EAAP Publ. 112.

Ouali, A., Herrera-Mendez, C., Coulis, G., Becila, S., Boudjellal, A., Aubry, L., et al. (2006). Revisiting the conversion of muscle into meat and the underlying mechanisms. *Meat Science, 74*(1), 44–58.

Pauly, H., & Schwan, H. P. (1959). Über die Impedanz einer Suspension von kugelförmigen Teilchen mit einer Schale. *Zeitschrift fur Naturforschung, 14b*, 125–131.

Pethig, R. (1979). *Dielectric and electronic properties of biological materials*. Chichester: John Wiley.

Pethig, R., & Kell, D. B. (1987). The passive electrical properties of biological systems: Their significance in physiology, biophysics and biotechnology. *Physics in Medicine and Biology, 32*, 933–970.

Pliquett, U., Altmann, M., Pliquett, F., & Schöberlein, L. (2003). Py – a parameter for meat quality. *Meat Science, 65*, 1429–1437.

Schwan, H. P. (1957). Electrical properties of tissue and cell suspensions. *Advances in biological and medical physics* (Vol. 5, pp. 147–209). New York: Academic Press.

Schwan, H. P., & Takashima, S. (1993). Electrical conduction and dielectric behavior in biological systems. *Encyclopedia of Applied Physics* (Vol. 5, pp. 177–200). Weinheim and New York: VCH Publishers.

Swatland, H. J. (1980). Anisotropy and postmortem changes in the electrical resistivity and capacitance of skeletal muscle. *Journal of Animal Science, 50*, 67–74.

Swatland, H. J. (1997). Observations on rheological, electrical and optical changes during rigor development in pork and beef. *Journal of Animal Science, 75*, 975–985.

Valentinuzzi, M. E., Morucci, J. P., & Felice, C. J. (1995). Bioelectrical impedance techniques in medicine. Part II: Monitoring of physiological events by impedance. *Critical Reviews in Biomedical Engineering, 24*, 353–466.

Valet, G., Silz, S., Metzger, H., & Ruhenstroth-Bauer, G. (1975). Electrical sizing of liver cell nuclei by the particle beam method. Mean volume, volume distribution and electrical resistance. *Acta Hepatogastroenterol (Stuttg), 22*(5), 274–281.

Varlan, A. R., & Sansen, W. (1996). Non-destructive electrical impedance analysis in fruit: Normal ripening and injuries characterization. *Electro-Magnetobiology, 15*, 213–227.

Whitman, T. A., Forrest, J. C., Morgan, M. T., & Okos, M. R. (1996). Electrical measurement for detecting early postmortem changes in porcine muscle. *Journal of Animal Science, 74*, 80–90.

Winger, R. J. (1979). *Conference on fibrous proteins*. London: Parry, D.A.D. & Creamer, L.K. Ed..

Wu, F. Y., & Smith, S. B. (1987). Ionic strength and myofibrillar protein solubilization. *Journal of Animal Science, 65*, 597–608.